

Investigating the effect of oxygen vacancy on the dielectric and electromechanical properties in ferroelectric ceramics

Veng-cheong Lo,^{1,a)} Winnie Wing-yee Chung,¹ Haixia Cao,^{1,2} and Xiao Dai²

¹*Department of Applied Physics, The Hong Kong Polytechnic University, Hung Hom, Kowloon, Hong Kong, People's Republic of China*

²*Department of Physics, Suzhou University, Suzhou, 215006, People's Republic of China*

(Received 11 April 2008; accepted 17 July 2008; published online 18 September 2008)

The effect of oxygen vacancy on the dielectric and electromechanical properties in lead titanate zirconate based ferroelectric ceramics is discussed in this paper. The presence of oxygen vacancy forms a defect-dipole inside a perovskite cell. This defect-dipole contributes to the unswitchable polarization and influences the alignment of the ferroelectric dipole in the same cell as well. The latter is due to the displacement of the *B*-site cation, which contributes to the switchable polarization. It is found that a double hysteresis emerges when the alignment of defect-dipole conforms with the crystal orientation, which is perpendicular to the measured polarization. Moreover, the optimal electromechanical property can be obtained by careful adjustment of *c*-domain volume fraction and the alignment of defect dipoles. Monte Carlo simulation based on the four-state Potts model is presented. Calculation results are compared with experiments. © 2008 American Institute of Physics. [DOI: 10.1063/1.2978376]

I. INTRODUCTION

Perovskite type ferroelectrics such as lead titanate zirconate [Pb(Ti_xZr_{1-x})O₃], barium titanate (BaTiO₃), and potassium sodium niobate [(K_{0.5}Na_{0.5})NbO₃] have been widely used for a large number of dielectric and electromechanical applications. Among these materials, both the dielectric and electromechanical properties rely on polarization switching, in which non-180° domain switching plays a dominant role.¹⁻⁴ On the other hand, in order to optimize the performance of these materials, a precise control on the material properties is vitally important. One typical factor is the presence of defects, which can be either point defects or dislocations. They are created in many different ways, such as non-stoichiometry, extrinsic doping,⁵ thermal mismatch, distortion upon phase transition, film/substrate lattice mismatch,⁶ etc. Among various types of defects, oxygen vacancies, either as isolated point defects or as defect—ion dipolar pairs by combining with other ionic species are always present in oxide ceramics. They are usually generated by annealing in oxygen—deficient ambient or lower valence cation substitution.

The role of oxygen vacancies on the ferroelectric properties has been extensively discussed before. For example, the presence of oxygen vacancies enhances the coercive field,^{7,8} creates imprint effect by shifting the polarization-electric field (*P*-*E*) loop along the electric field axis,^{7,9} and causes polarization fatigue effect.^{10,11} There are also a number of reports on the occurrence of double hysteresis loops in the presence of oxygen vacancies.⁹⁻¹³ Ren¹⁴ has presented a qualitative explanation for the presence of double hysteresis loop by considering the conformal alignment of defect dipoles along the spontaneous polarization *P*_S direction im-

posed by the crystal symmetry. Each of these dipoles is created by oxygen vacancy in the perovskite cell. The measured polarization driven by an external electric field is perpendicular to *P*_S. It was also suggested that the alignment of these defect dipoles is achieved after aging. Furthermore, this defect dipole also influences the rotation of the ferroelectric dipole of the same cell. The latter will, in turn, affect both the overall polarization and electromechanical response.

It is interesting to know how the electromechanical property is influenced by oxygen vacancies. Several aspects may be studied, such as the domain structure in the presence of oxygen vacancies, coupling between the oxygen vacancy and the ferroelectric dipole, strain effect due to lattice distortion, change in grain size due to lower valence doping, etc. For instance, Fan *et al.*¹⁵ have observed different domain structures of Pb[(Zn_{1/3}Nb_{2/3})_{0.5}-(Zr_{0.47}Ti_{0.53})_{0.5}]O₃ (PZN-PZT) samples prepared under different conditions: as-sintered, postannealed in argon, and postannealed in oxygen ambient atmospheres. The quantities of oxygen vacancies are believed to be different among these samples. It was found that the sample annealed in oxygen atmosphere exhibited the largest electromechanical coupling factor and piezoelectric coefficient, while the as-sintered one showed the least. In other words, the electromechanical effect is reduced in the presence of oxygen vacancies. Zhang and Ren⁸ have drawn similar conclusions by suggesting that the domain wall motion through 90° rotation is impeded because of the unfavorable alignment of ferroelectric dipoles in the presence of defect dipoles generated by oxygen vacancies. However, Hou *et al.*¹⁶ have shown that maximum electromechanical coupling factor *k*_p as well as piezoelectric coefficient *d*₃₃ is obtained by 1% doping of MnO₂ in Pb[(Zn_{1/3}Nb_{2/3})_{0.20}-(Zr_{0.50}Ti_{0.50})_{0.80}]O₃ ceramics. Further incorporation of MnO₂ reduces these two parameters. They suggested that MnO₂ doping not only increases the quantity of oxygen va-

^{a)}Author to whom correspondence should be addressed. Electronic mail: timothy.lo@polyu.edu.hk.

cancies, but also influences the crystal structure and microstructure. The increase in electromechanical properties in the presence of oxygen vacancies suggests that the latter is not necessarily a detrimental factor on the device performance. Furthermore, their effects on the microstructure as well as their role on the polarization switching should be explored.

The role of dislocations on the ferroelectric properties has also been studied. For instance, Alpay *et al.*¹⁷ have performed theoretical investigation using thermodynamic analysis. The coupling between the dislocation-induced stress and polarization results in polarization gradient near the dislocation. The polarization gradient reduces the polarization in a region over several nanometers. This in turn imposes a critical thickness below which the ferroelectricity is unstable. Similarly, Balzar *et al.*¹⁸ have derived the shift in Curie–Weiss temperature in the presence of inhomogeneous strain using thermodynamic Gibbs free energy approach. They attributed the inhomogeneous strain to misfit dislocations, threading dislocations, and nonrandomly distributed point defects. However, either the inhomogeneity in strain or in polarization does not necessarily deteriorate the material properties. For instance, Zhong *et al.*¹⁹ have observed enhanced piezoelectric response in multilayered and heterogeneous $\text{Ba}_{1-x}\text{Sr}_x\text{TiO}_3$ thin films and in compositionally graded $\text{BaTiO}_3\text{--Ba}_{1-x}\text{Sr}_x\text{TiO}_3$ and $\text{PbTiO}_3\text{--Pb}_{1-x}\text{Zr}_x\text{TiO}_3$ systems.²⁰

In this work, we try to investigate the coupling effect of oxygen vacancy with the ferroelectric dipole of each perovskite cell. The theoretical modeling and numerical simulation are presented in next section. The simulation results are presented in Sec. III.

II. THEORY AND MODELING

In this work, we are investigating the dielectric and electromechanical properties of a lead titanate zirconate $\text{Pb}(\text{Ti}_{1-x}\text{Zr}_x)\text{O}_3$ (PZT) single crystal in tetragonal phase. The crystal is in multidomain configuration, where the polarization of *c*-domain is along the *z*-axis (or longitudinal axis), and *a*-domain along either *x*- or *y*-axis (or transverse axis). Due to the equivalence between the two transverse directions, it is desirable to simply the system into a two-dimensional one in order to reduce the computation. Consequently, we adopt a two-dimensional four-state Potts model

with N_x and N_z perovskite cells along *x* and *z* directions, respectively. The width and thickness of the sample are $w = N_x\Delta$ and $d = N_z\Delta$, respectively, where Δ is the size of a cell. The use of Potts model enables us to simulate the interaction of oxygen vacancy in each cell, the ferroelastic response in a 90° dipolar rotation, and the association between the ferroelectric dipoles and ferroelastic strain states. The detailed description of this model can be referred to the previous publications.^{7,21} A ferroelectric dipole at a cell is a result of the displacement of the *B*-site cation from the center of symmetry. In the tetragonal phase under the two-dimensional geometry, it has four different states denoted by the following pseudospin matrices:

$$\begin{aligned}\hat{S}_{i,j} = \hat{S}_a &= \begin{pmatrix} 1 \\ 0 \end{pmatrix}, & (\text{along } +z \text{ direction}), \\ \hat{S}_{i,j} = \hat{S}_b &= \begin{pmatrix} 0 \\ 1 \end{pmatrix}, & (\text{along } +x \text{ direction}), \\ \hat{S}_{i,j} = \hat{S}_c &= \begin{pmatrix} -1 \\ 0 \end{pmatrix}, & (\text{along } -z \text{ direction}), \\ \hat{S}_{i,j} = \hat{S}_d &= \begin{pmatrix} 0 \\ -1 \end{pmatrix}, & (\text{along } -x \text{ direction}),\end{aligned}\quad (1)$$

where $0 < i \leq N_x$ and $0 < j \leq N_z$ represent the position of the cell in the crystal. Likewise, if an oxygen vacancy exists in a cell, it can be located at one of the four faces. The vacancy states can be described by the following matrices:

$$\hat{V}_{i,j} = \begin{cases} \begin{pmatrix} 0 \\ 0 \end{pmatrix} & \text{absent} \\ \begin{pmatrix} 1 \\ 0 \end{pmatrix} & \text{top} \\ \begin{pmatrix} 0 \\ 1 \end{pmatrix} & \text{bottom} \\ \begin{pmatrix} 0 \\ -1 \end{pmatrix} & \text{right} \\ \begin{pmatrix} 0 \\ 1 \end{pmatrix} & \text{left} \end{cases} = \begin{cases} \begin{pmatrix} -1 \\ 0 \end{pmatrix} & \text{bottom} \\ \begin{pmatrix} 0 \\ -1 \end{pmatrix} & \text{right} \end{cases}, \quad (2)$$

where the zero matrix represents the absence of vacancy. The number of vacancies in the system is N_V , where $N_V < N_x N_z$. In the presence of the top and bottom surfaces, the distribution of oxygen vacancies along the thickness direction is given by

$$f_V(z) = \frac{1}{\Delta} \left(\frac{N_V}{N_x} \right) \frac{\exp(-z/Lz_1) + \exp[-(d-z)/Lz_2]}{Lz_1[1 - \exp(-d/Lz_1)] + Lz_2[1 - \exp(-d/Lz_2)]}, \quad (3)$$

where Lz_1 and Lz_2 are characteristic distribution lengths of oxygen vacancies at the top and bottom surfaces. Note that when $Lz_1 = Lz_2 \gg d$, the distribution becomes uniform given by $f_V(z) = N_V/wd$. Furthermore,

$$\int_0^w \left[\int_0^d f_V(z) dz \right] dx = N_V. \quad (4)$$

The probabilities of the oxygen vacancy at the different positions of a cell are denoted by p_T , p_L , p_B , and p_R corresponding to the top, left, bottom, and right faces, respectively, i.e., associated with the vacancy states $\hat{V}_{i,j}$ of Eq. (2). It is also restricted that $p_T + p_L + p_B + p_R = 1$. We will discuss the effect of oxygen vacancy in the following paragraph.

First of all, an oxygen vacancy is created by the removal

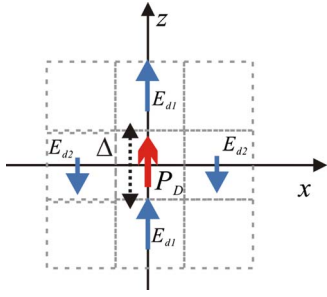


FIG. 1. (Color online) Local electric fields induced in the neighboring cells in the presence of a defect dipole formed by an oxygen vacancy at the top face of the cell.

of an oxygen ion in one of the faces of the perovskite cell. It is positively charged and forms a defect-dipole P_D with the direction pointing from the cell center toward the vacancy, even without other doping species. On one hand, the B -site cation in the same cell, such as Ti^{4+} , will displace away from the vacancy site and result in a ferroelectric dipole antiparallel to the defect dipole due to the Columbic repulsion between Ti^{4+} and the oxygen vacancy.^{7,21} This effect can be represented by the additional Hamiltonian term

$$H_a = H_{V1} \hat{V}_{i,j}^T \hat{S}_{i,j}, \quad (5)$$

where H_{V1} is the coupling coefficient and the superscript T after a generic matrix \hat{X} denotes the transpose matrix of \hat{X} . H_{V1} bears a positive sign, reflecting that the antiparallel alignment between the two dipoles is preferred.

Second, in the presence of a defect-dipole P_D , local electric fields in the neighboring cells are induced, as shown in Fig. 1. The magnitudes of these fields at the nearest neighbors are

$$E_{d1} = \frac{2P_D \Delta}{4\pi\epsilon_0(\Delta - b/2)^2(\Delta + b/2)^2} \quad (6)$$

and

$$E_{d2} = \frac{P_D}{4\pi\epsilon_0(\Delta^2 + b^2/4)^{3/2}}, \quad (7)$$

where b is the distance of the oxygen vacancy away from the center of the cell. The dipole field drops rapidly by the $1/r^3$ dependence. The induced field at the second nearest neighbors or beyond can thus be ignored. Conversely, defect dipole induced fields from the four nearest neighbors of a cell located at (i, j) can be obtained by the following relations:

$$\hat{E}_{i,j}^V = \begin{pmatrix} E_{d1}(\hat{V}_{i,j-1,z} + \hat{V}_{i,j+1,z}) - E_{d2}(\hat{V}_{i-1,j,z} + \hat{V}_{i+1,j,z}) \\ -E_{d2}(\hat{V}_{i,j-1,x} + \hat{V}_{i,j+1,x}) + E_{d1}(\hat{V}_{i-1,j,x} + \hat{V}_{i+1,j,x}) \end{pmatrix}, \quad (8)$$

where $\hat{V}_{m,n,z}$ and $\hat{V}_{m,n,x}$ are the z - and x -components (or first and second row), respectively, of the matrix $\hat{V}_{m,n}$ located at a position (m, n) .

The presence of oxygen vacancy also induces a local tensile stress on the same cell. Uchida *et al.*²² have observed the presence of residual tensile stress in Pb-poor $PbTiO_3$ film where lead and oxygen vacancies exist. Gupta and Katiyar²³

have investigated the lattice optical phonons in strontium titanate thin films using Raman spectroscopy. They concluded that development of microstress/strain was possibly due to the incorporation of defects such as oxygen vacancies. Though the system they have studied is strontium titanate, which is in cubic phase at room temperature, it has a perovskite structure. There are also reports on the presence of local strain fields at the proximity of mismatch dislocations.⁶ The vacancy-induced stress can be described by the following expression:

$$\hat{\sigma}_{i,j}^V = \begin{cases} \begin{pmatrix} \sigma_1 \\ 0 \\ 0 \end{pmatrix} & \text{for vacancy at the top or bottom face} \\ \begin{pmatrix} 0 \\ \sigma_1 \\ 0 \end{pmatrix} & \text{for vacancy at the left or right face,} \end{cases} \quad (9)$$

where $\sigma_1 > 0$ is a constant stress. It is noted from Eq. (9) that this stress is longitudinal if the vacancy is at the top or bottom face or transverse if the vacancy is at the left or right face.

The system Hamiltonian is given by the following expression:

$$H = -J \sum_{i,j,k,l} \hat{S}_{i,j}^T \hat{S}_{k,l} - P_S \sum_{i,j} \hat{E}_{i,j}^T \hat{S}_{i,j} - \sum_{i,j} \hat{\sigma}_{i,j}^T \hat{\epsilon}_{i,j} - \alpha \sum_{i,j,k,l} \hat{\epsilon}_{i,j}^{F,T} \hat{\epsilon}_{k,l}^F + H' + H_a, \quad (10)$$

where J is the coupling coefficient between the neighboring ferroelectric dipoles, P_S the saturation polarization, $\hat{\sigma}_{i,j}$ the strain at each cell, α the coupling coefficient between neighboring ferroelastic strain states. The term H' caters for the effect of anisotropic switching of dipoles through 90° rotation,²¹ which can be expressed as

$$H' = - \sum_{i,j} h_{CA} (\phi_C - \phi_A) |\hat{n}^T \hat{S}_{i,j}|, \quad (11)$$

where h_{CA} is the energy barrier for switching a ferroelectric dipole from c - to a -domain, ϕ_C and $\phi_A = 1 - \phi_C$ are volume fractions of c -domains and a -domains, respectively, \hat{n} is a longitudinal unit matrix, given by $\hat{n} = \begin{pmatrix} 1 \\ 0 \\ 0 \end{pmatrix}$. The last term in Eq. (10) H_a incorporates the effect of oxygen vacancy, as discussed in Eq. (5). It is assumed that only oxygen vacancy-induced stress given by Eq. (10) exists and there is no external stress, so that $\hat{\sigma}_{i,j} = \hat{\sigma}_{i,j}^V$. Moreover, this internal stress is inhomogeneous in space but constant in time. A uniform periodic external alternating electric field is applied along the longitudinal direction and the total electric field is given by

$$\hat{E}_{i,j} = \hat{E}_{\text{ext}}(t) + \hat{E}_{i,j}^V. \quad (12)$$

Finally, the strain in each cell can be divided into three contributions: ferroelastic strain $\hat{\epsilon}_{i,j}^{F,F}$ associated with the rotation of a ferroelastic dipole, elastic strain $\hat{\epsilon}_{i,j}^{\text{el}}$ governed by the elastic property of the sample, and field-induced strain $\hat{\epsilon}_{i,j}^{\text{FI}}$ attributed to the distortion of cell due to the charge separation. The last strain component is related to the electric field

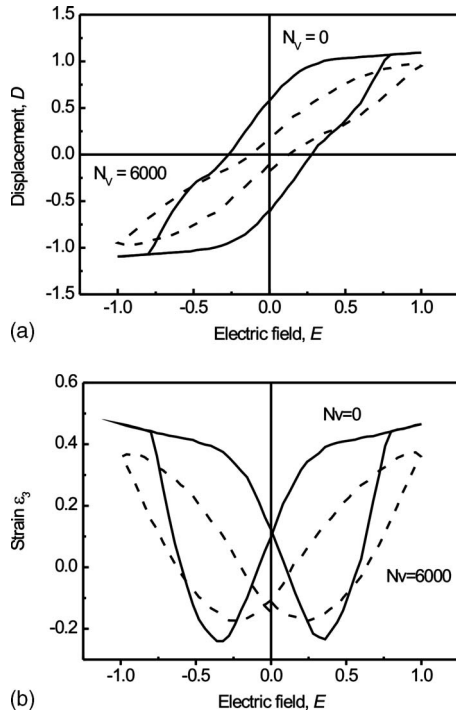


FIG. 2. (a) Displacement vector–electric field (D - E) hysteresis loops and (b) Longitudinal strain–electric field (ϵ_3 - E) butterfly loops under two different amounts of oxygen vacancies: $N_V=0$ (solid curve) and $N_V=6000$ (dashed curve).

via the piezoelectric (d_{33} and d_{31}) and electrostrictive coefficients (q_{333} and q_{331}). The explicit expressions of these strain components have been discussed before.²¹

In the present calculation, it is assumed that the sample is initially unpoled and divided into a number of domains randomly aligned with the four different orientations. Furthermore, the vacancy species are immobile. The ensemble of dipoles $\{\hat{S}_{ij}\}$ then evolves in time according to the Metropolis algorithm. The overall polarization and strain at each time instance are evaluated by their ensemble averages, such as

$$P = \frac{P_s \sum_{i,j} \{\hat{n}^T \hat{S}_{ij}\}}{N_x N_z} \quad (13)$$

and

$$\epsilon_3 = \frac{1}{N_x N_z} \sum_{i,j} \hat{n}^T (\hat{\epsilon}_{i,j} - \hat{\epsilon}_{i,j}^0). \quad (14)$$

III. RESULTS AND DISCUSSION

The double hysteresis loop and the electromechanical property induced by oxygen vacancies are simulated. The displacement vector–electric field (D - E) loops and strain–electric field (ϵ_3 - E) butterfly loops in the presence and absence of oxygen vacancies are then compared, as shown in Figs. 2(a) and 2(b). The presence of oxygen vacancies is characterized by $N_V=6000$, while $N_V=0$ in their absence. They are denoted by dashed and solid lines, respectively. It is observed that the double hysteresis loop and the reduction of

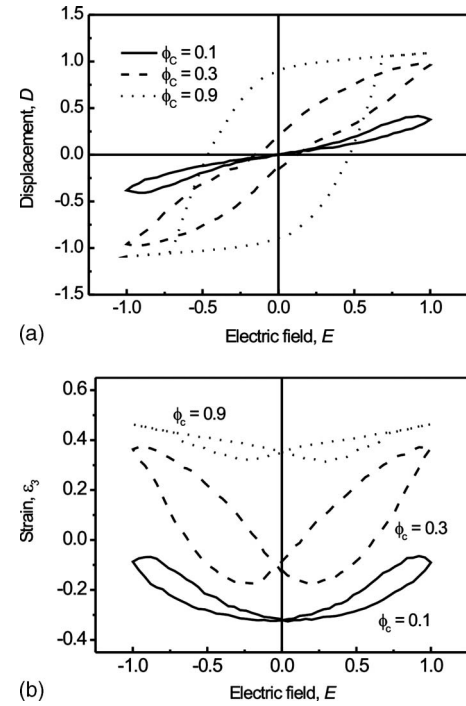


FIG. 3. Effect of the c -domain volume fractions ϕ_C on (a) D - E hysteresis loop and (b) ϵ_3 - E butterfly loop. The values of ϕ_C are 0.1 (solid), 0.3 (dashed), and 0.9 (dotted), respectively. The vacancy profile remains unchanged among these curves: $p_T=p_B=0.10$ and $p_L=p_R=0.40$.

butterfly loop occur in the presence of oxygen vacancies. The numerical parameters used for this simulation are magnitude of the alternating electric field $E_0=1.0$, frequency=400, temperature $T=1.2$, Young's modulus=2, Poisson ratio=0.3, $P_s=1$, piezoelectric coefficients $d_{33}=0.02$, and $d_{31}=-0.01$, electrostrictive coefficients $q_{333}=0.05$ and $q_{331}=-0.025$, $E_{d1}=1.5$, $E_{d2}=0.2$, $\sigma_1=0.5$, $h_{CA}=1.0$, $\phi_C=0.3$, $p_T=p_B=0.10$, and $p_L=p_R=0.40$.

The effects of the c -domain volume fraction and hence the anisotropic switching on the hysteresis and butterfly loops are shown in Figs. 3(a) and 3(b), respectively. The vacancy profile in these graphs is the same as for Figs. 2(a) and 2(b). At low ϕ_C value, most of the ferroelectric dipoles are preferentially aligned along the transverse (or 100) direction at small electric field. They can be switched to longitudinal (or 001) direction only when the electric field is very large, resulting in a double hysteresis loop. Moreover, the loop area depends on the ability of ferroelectric switching through 90° rotation of these dipoles. Consequently, the larger the ϕ_C value gives rise to the larger loop area as the switching becomes easier. On the other hand, the strain–electric field butterfly loop is largest at some moderate ϕ_C value. At low ϕ_C , most of the ferroelectric dipoles are clamped along the transverse direction, and only a few of them can be switched toward the longitudinal direction even at a very high electric field. It results in a small longitudinal strain. On the contrary, at a high ϕ_C value, these dipoles are automatically aligned along the longitudinal direction. The application of electric field only flips them from one longitudinal direction to the other. It creates a large change in polarization but a small change in longitudinal strain.

The vacancy distribution at different faces of a cell, as

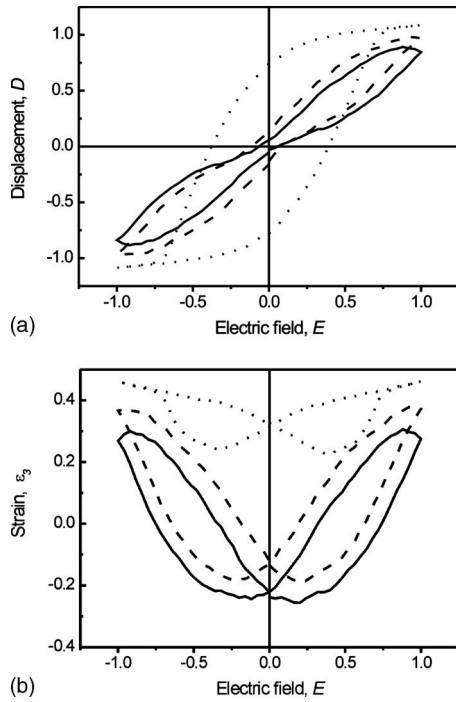


FIG. 4. Effect of probabilities of an oxygen vacancy at different positions of a cell on (a) D - E hysteresis loop and (b) ϵ_3 - E butterfly loop. The vacancy profiles for these curves are (i) $p_T=p_B=0.05$, $p_L=p_R=0.45$ (solid), (ii) $p_T=p_B=0.10$, $p_L=p_R=0.40$ (dashed), and (iii) $p_T=p_B=0.45$, $p_L=p_R=0.05$ (dotted). The c -domain volume fraction for all cases is $\phi_c=0.3$.

characterized by the corresponding probabilities, also influences the alignment of ferroelectric dipoles. Its effects on the hysteresis and butterfly loops are manifested in Figs. 4(a) and 4(b), respectively. For small p_T and p_B values (or equivalently large p_L and p_R values), as denoted by solid and dashed lines, most of the vacancies are on the left or right faces of the cell, while few of them are on the top or bottom faces. Consequently, this configuration encourages the transverse alignment for the ferroelectric dipoles. It has a similar effect as in the low ϕ_c case, i.e., the emergence of double hysteresis loops and the downward shifting of the butterfly loops. At high p_T and p_B values, as denoted by the dotted line, ferroelectric dipoles are preferentially aligned along the longitudinal direction. The double hysteresis loop disappears and is replaced by an ordinary one. Similarly, the butterfly loop area is also reduced because most of the ferroelectric dipoles are already along the longitudinal direction, irrespective of the electric field. The loop area depends on the fraction of dipoles undergoing 90° rotation. A large fraction results in the large loop area and vice versa. A strong clamping of ferroelectric dipoles along the transverse direction or their preferential alignment along the longitudinal direction results in a small fraction. On the contrary, a large fraction can be obtained under the following condition. The ferroelectric dipoles are preferentially aligned along the transverse direction and are switchable by the application of a longitudinal electric field. The electromechanical property is governed by the butterfly loop area. The piezoelectric coefficient can be determined by $d_{33}=\Delta\epsilon_3/\Delta E$, where $\Delta\epsilon_3$ is the change in longitudinal strain over a cycle and ΔE the change in electric field. The presence of oxygen vacancies does not necessarily

reduce the area. As introduced earlier, the alignment of these defect dipoles along the transverse direction dictates the amount of ferroelectric dipoles that can be switched through 90° rotation. It has been shown before that the electromechanical effect is predominantly contributed by 90° rotations.¹⁻⁴ Thus the vacancy profile can strongly influence the electromechanical property. Hou *et al.*¹⁶ have carefully controlled the amount of oxygen vacancies in their experimental investigation on 0–3 wt % MnO_2 -doped $\text{Pb}[(\text{Zn}_{1/3}\text{Nb}_{2/3})_{0.20}-(\text{Zr}_{0.50}\text{Ti}_{0.50})_{0.80}]\text{O}_3$ system and obtained an optimal electromechanical response by 1% MnO_2 doping. Zhang *et al.*²⁴ have also obtained similar enhanced electromechanical properties in MnO_2 -doped $(\text{Ba}_{0.95}\text{Sr}_{0.05})\text{TiO}_3$ ceramics. From both of these experiments, MnO_2 is an acceptor dopant, creating oxygen vacancies.

In this simulation work, it is assumed that oxygen vacancies are symmetrically distributed with respect to the top and bottom faces, as well as left and right faces. Any asymmetric distribution of oxygen vacancies over a cell (i.e., $p_T \neq p_B$ or $p_L \neq p_R$) or over the sample (i.e., $L_{z1} \neq L_{z2}$) results in the shift of the hysteresis loops, which is conventionally known as imprint effect. However, the asymmetric distribution of oxygen vacancies is beyond our present discussion.

From the simulation results, it can be concluded that the existence of double hysteresis loop is attributable to the conformational alignments of ferroelectric dipoles and the defect dipoles along the transverse direction. When these two alignments are mutually perpendicular, the effect induced by one of them might be cancelled out by the other and only an ordinary hysteresis loop can be obtained. This result is consistent with the conclusion drawn by Ren and Zhang^{8,14} after their investigation on the aged BaTiO_3 samples. They suggested that oxygen vacancies were generated by lower valence doping such as MnO . After aging these samples, the diffusion of oxygen vacancies results in symmetry-conforming property, in which the alignment of the defect-dipoles conforms with the direction of the spontaneous polarization. Both the measured polarization and driving electric field are perpendicular to the former alignments. Even though their system was BaTiO_3 while our present case is $\text{Pb}(\text{Ti}_{1-x}\text{Zr}_x)\text{O}_3$, both of them have identical crystal structure and of the same displacive-type ferroelectricity. The direction of spontaneous polarization in a tetragonal cell is along its elongated axis. If this axis is along the transverse (or 100) direction, then the sample is dominated by a -domains with a small ϕ_c value. However, a small ϕ_c value alone is not enough to produce the double hysteresis loop, as depicted by the dotted line in Fig. 4(a). In this case, defect dipoles are predominately along the longitudinal direction (with large p_T and p_B values). These defect dipoles encourage the longitudinal alignment of ferroelectric dipoles, canceling out the effect of small ϕ_c value. Similarly, the transverse defect dipoles alone do not result in double hysteresis loop. For instance, the dotted line in Fig. 3(a) represents the case where most of the defect dipoles are transversely aligned, the D - E relation is restored to an ordinary hysteresis loop under a large ϕ_c value. In summary, a double hysteresis loop occurs only when the defect-dipole alignment conforms with the direction of the spontaneous polarization, which is

determined by the crystal orientation and structure, consistent with the conclusion drawn by Ren¹⁴ and Zhang.⁸ Warren *et al.*²⁵ have confirmed the preferential alignment of defect dipole along the spontaneous polarization direction in BaTiO₃ and Pb(Ti_{1-x}Zr_x)O₃ samples upon aging, using electron paramagnetic resonance investigation.

IV. CONCLUSION

The role of oxygen vacancy in the switching mechanism of lead titanate zirconate based ceramics is discussed and the numerical simulation using four-state Potts model is presented. A defect dipole is induced in the presence of an oxygen vacancy in a cell. Its location in the cell strongly influences the switching behavior of the ferroelectric dipole. The latter in turn influences the dielectric and electromechanical properties. A double hysteresis loop can be generated if the alignment of defect dipoles conforms with the direction of spontaneous polarization, which is perpendicular to the direction of measured polarization and driving electric field. Moreover, enhanced electromechanical properties can also be obtained by optimizing the orientations of the crystal and the defect dipoles.

ACKNOWLEDGMENTS

This work is financially supported by the research grant from The Hong Kong Polytechnic University under Grant No. A-PA8W.

¹R. Yimnirun, Y. Laosiritaown, and S. Wongsanmai, *J. Phys. D* **39**, 759 (2006).

²D. Zhou, M. Kamlah, and D. Munz, *J. Eur. Ceram. Soc.* **25**, 425 (2005).

³V. Nagarajan, I. G. Jenkins, S. P. Alpay, H. Li, S. Aggarwal, L. Salamanca-Riba, A. L. Roytburd, and R. J. Ramesh, *J. Appl. Phys.* **86**, 595 (1999).

⁴L.-F. Wang and J.-M. Liu, *Appl. Phys. Lett.* **90**, 062905 (2007).

⁵B. Guiffard, D. Audigier, L. Lebrun, M. Troccaz, and E. Pleska, *J. Appl. Phys.* **86**, 5747 (1999).

⁶I. B. Misirlioglu, S. P. Alpay, F. He, and B. O. Wells, *J. Appl. Phys.* **99**, 104103 (2006).

⁷V. C. Lo, *J. Appl. Phys.* **92**, 6778 (2002).

⁸L. Zhang and X. Ren, *Phys. Rev. B* **73**, 094121 (2006).

⁹T. Friessnegg, S. Aggarwal, R. Ramesh, B. Nielsen, E. H. Poindexter, and D. J. Keeble, *Appl. Phys. Lett.* **77**, 127, (2000).

¹⁰K. T. Li and V. C. Lo, *J. Appl. Phys.* **97**, 034107, (2005).

¹¹M. Dawber and J. F. Scott, *Appl. Phys. Lett.* **76**, 1060 (2000).

¹²Q. Tan, Z. Xu, and D. Viehland, *J. Mater. Res.* **14**, 465 (1999).

¹³I. W. Kim, D. S. Lee, S. H. Kang, and C. W. Ahn, *Thin Solid Films* **441**, 115 (2003).

¹⁴X. Ren, *Nat. Mater.* **3**, 91 (2004).

¹⁵H. Fan, G.-T. Park, J.-J. Choi, and H.-E. Kim, *Appl. Phys. Lett.* **79**, 1658 (2001).

¹⁶Y. Hou, M. Zhu, F. Gao, H. Wang, B. Wang, H. Yan, and C. Tian, *J. Am. Ceram. Soc.* **87**, 847 (2004).

¹⁷S. P. Alpay, I. B. Misirlioglu, V. Nagarajan, and R. Ramesh, *Appl. Phys. Lett.* **85**, 2044 (2004).

¹⁸D. Balzar, P. A. Ramakrishnan, and A. M. Hermann, *Phys. Rev. B* **70**, 092103 (2004).

¹⁹S. Zhong, Z.-G. Ban, S. P. Alpay, and J. V. Mantese, *Appl. Phys. Lett.* **89**, 142913 (2006).

²⁰R. Nath, S. Zhong, S. P. Alpay, B. D. Huey, and M.W. Cole, *Appl. Phys. Lett.* **92**, 012916 (2004).

²¹V.-C. Lo, W. W.-Y. Chung, and S. C.-K. Chow, *J. Appl. Phys.* **101**, 114111 (2007); H.-X. Cao, V.-C. Lo, and W. W.-Y. Chung, *ibid.* **99**, 024103, (2006).

²²H. Uchida, T. Kiguchi, N. Wakiya, K. Shinozaki, and N. Mizutani, *Korean J. Ceram.* **6**, 385 (2000).

²³S. Gupta and R. S. Katiyar, *J. Raman Spectrosc.* **32**, 885 (2001).

²⁴L. X. Zhang, W. Chen, and X. Ren, *Appl. Phys. Lett.* **85**, 5658 (2004).

²⁵W. L. Warren, G. E. Pike, K. Vanheusden, D. Dimos, and B. A. Tuttle, *J. Appl. Phys.* **79**, 9250 (1996).